Pattern formation of a step induced by a moving linear source

Shinji Kondo,[1] Masahide Sato,[2] Makio Uwaha,[1,*] and Hiroki Hibino[3]

[1]*Department of Physics, Nagoya University, Furo-cho, Chikusa-ku, Nagoya 464-8602, Japan*

[2]*Information Media Center, Kanazawa University, Kakuma-machi, Kanazawa 920-1192, Japan*

[3]*Materials Science Laboratory, NTT Basic Research Laboratories, NTT Corporation, 3-1 Morinosato-Wakamiya, Atsugi, Kanagawa 243-0198, Japan*

(Received 17 January 2011; revised manuscript received 12 April 2011; published 11 July 2011)

By means of Monte Carlo simulation with a square lattice model, we study pattern formation of a step induced by a moving linear source of adatoms. Incorporation of adatoms, which are released from a linear source in front of the straight step, causes wandering instability of the step during growth. In contrast to the usual wandering pattern, a treelike step follows the source so that a steadily growing state is realized. Branching occurs frequently in growth toward the [01] direction, while branching is suppressed in growth toward the [11] direction. The characteristic wavelength (period of branches) λ of the pattern is determined by velocity V_p of the linear source and step stiffness $\tilde{\beta}$ as $\lambda \sim \sqrt{\Gamma l_\mathrm{D}}$ ($l_\mathrm{D} = D_\mathrm{s}/V_\mathrm{p}$, the diffusion length defined by diffusion coefficient D_s and V_p; Γ, the capillary length proportional to $\tilde{\beta}$). A comblike step pattern is formed in the [11] growth. The pattern is similar to that observed on a Si(111) surface under Ga deposition. If source velocity V_p is increased, characteristic length λ becomes shorter to follow the source. With V_p above a critical velocity, the step grows at the critical velocity independent of V_p and shows a fractal-like pattern. The critical velocity is related to the fractal dimension of the diffusion-limited aggregation. Similarity of the comblike pattern to a finger pattern observed in graphene growth is also discussed.

DOI: 10.1103/PhysRevB.84.045420 PACS number(s): 81.10.Aj, 05.70.Ln, 47.20.Hw, 68.35.Fx

I. INTRODUCTION

Atomic steps on a crystal surface show various types of pattern formation during growth, during sublimation, and under the influence of an external field.[1,2] In growth, if the diffusion barrier at a step edge[3–5] is present, a higher flux of adsorbed atoms (adatoms) attach from the lower side terrace than from the upper side terrace, and the step becomes unstable.[6] Wandering instability is generally possible with a supply of adatoms from the forward direction. The motion of a destabilized step is chaotic[7,8] and is characterized by the Kuramoto-Sivashinsky equation.[9,10] With a strong crystal anisotropy, the chaotic behavior is suppressed, and a regular periodic pattern appears.[11] During growth without evaporation of adatoms, an array of straight steps shows a regular in-phase wandering pattern, and the amplitude of wandering is increased with time.[12,13] It is a typical wandering pattern in conservative systems.[14–16] In sublimation, the drift of adatoms driven by an external field[17] also induces step wandering.[18,19] The pattern may be either chaotic or regular, depending on the symmetry of the system determined by the drift direction.[20]

Recently, a type of wandering pattern was found on a Ga-deposited Si(111) vicinal surface.[21] When Ga is deposited at about 580 °C, the 7×7 structure is transformed to the $\sqrt{3} \times \sqrt{3}$ structure first. Further deposition of Ga transforms the $\sqrt{3} \times \sqrt{3}$ structure to the 6.3×6.3 structure in which the density of Si atoms in the top surface layer is about half that of the former structure. The excess Si atoms are emitted onto the surface during the transformation at the phase boundary moving with Ga deposition. The excess adatoms on the terrace form a growing new layer at the step. The transformation preferentially occurs in the vicinity of the lower side of the existing steps. Thus, Si atoms are supplied to the step from the lower side, and a wandering instability is induced. The protruding part of the step grows like a finger, and the whole pattern is like a comb (Fig. 1). In Ref. 21, it is suggested that the pattern is induced by the moving phase boundary, which is acting as a linear source of atoms in front of the step. Although the mechanism of the instability seems similar to that of the above-mentioned wandering instabilities,[6–8] the resulting pattern is not similar to the known ones at all. Since similar situations with a moving source of atoms may occur in other systems, we study pattern formation of a step induced by a guiding linear source of adatoms.

II. MODEL

We consider a lattice model in Monte Carlo (MC) dynamics. The original model for a usual growing surface is described in Ref. 8. The system consists of a square lattice substrate, adatoms diffusing on the substrate, an inactive layer of solid atoms on the substrate, and active step atoms that form an edge of the solid layer (Fig. 2). In the present model, a solid atom and an adatom are distinguished as different states, and a step atom is an active solid atom. In this paper, the transformation from an adatom to a step atom is called solidification, and the opposite process is called melting.

In Fig. 2, the solid layer is located at the bottom, and a linear source of adatoms, which represents a straight phase boundary in the Si system, is at the top. Adatoms are present on the terrace between the step and the linear source.

In a MC trial, we randomly choose one of the active atoms, i.e., adatoms and step atoms. When an adatom is chosen, a diffusion trial is performed. The adatom moves randomly to one of the four neighboring sites if the chosen site is empty. After the diffusion trial, if the adatom happens to be in contact with a step atom, a solidification trial is performed.

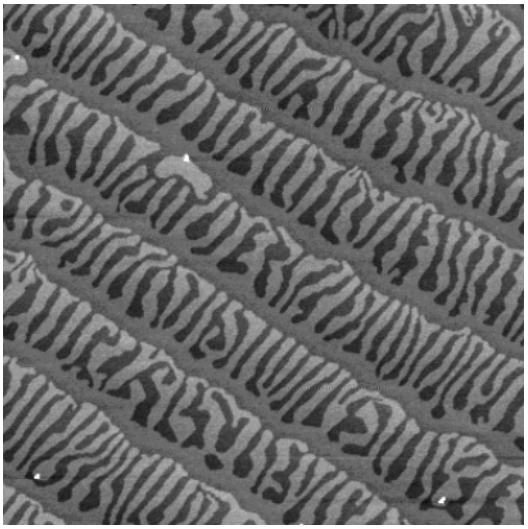

FIG. 1. A comblike step pattern on a Si(111) vicinal face under Ga deposition at 603 °C. The view is 3 μm × 3 μm.

The solidification probability p_+ is given by

$$p_+ = \frac{1}{1 + e^{(\Delta E - \phi)/k_B T}}, \tag{1}$$

where ΔE is the change in step energy (the kink energy, or half the lateral bond energy, ϵ times the perimeter length in the unit of the lattice constant) associated with the solidification, and ϕ is the energy gain in solidification.[22] When a step atom is chosen instead of an adatom, a melting trial is performed. The melting probability p_- is given by

$$p_- = \frac{1}{1 + e^{(\Delta E + \phi)/k_B T}}, \tag{2}$$

where ΔE is the change in step energy associated with the melting. Time in the simulation is increased with each diffusion trial by $(4N_{ad})^{-1}$, where N_{ad} is the number of adatoms so that the diffusion coefficient is set to be unity.

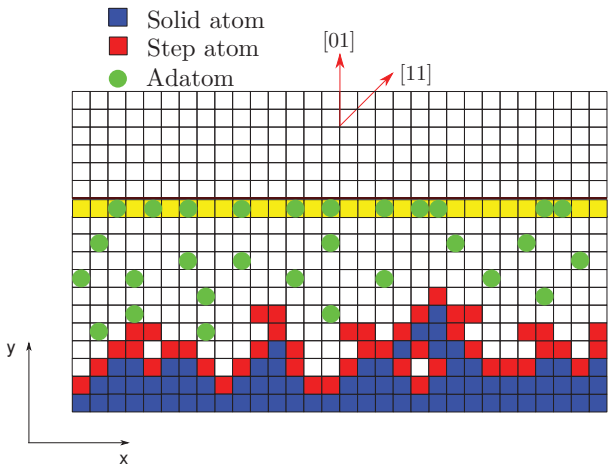

FIG. 2. (Color online) The lattice model for a (01) step. The blue (darkest gray) and red (dark gray) squares are solid and step atoms. The green (gray) circles are adatoms. The yellow (light gray) squares are the phase boundary.

A step and a straight linear source of adatoms are located on a square lattice, perpendicular to (01) or (11) orientation. [See Fig. 2 for a (01) step. For a (11) step, the square lattice is rotated by 45°.] Initially, the step is straight, and the position of the linear source is next to the step in the lower side. For the motion of the linear source, every time interval $(V_p)^{-1}$, a new single row of the lattice with randomly distributed c_0 adatoms per site is added at the top of the system. The boundary condition in the x direction (horizontal direction) is periodic, and that at the top is reflecting: Adatoms only move between the source and the step.[23] The linear source moves forward in the y direction at constant velocity V_p, releasing adatoms. The density of adatoms released at the phase boundary is set to $c_0 = 0.525$ (we choose the lattice constant as the length unit) except for Fig. 9. In our simulation, the equilibrium adatom density is $c_{eq}^0 = 0.05$, which is determined by the energy gain $\phi/k_B T = 3.0$ in solidification as $c_{eq}^0 = e^{-\phi/k_B T}$. Therefore, half the system is covered by a solid in the long run.[24] The maximum system size of most simulations is 1024 × 2000, and all data shown are averaged over at least ten independent runs.

III. SIMULATION RESULT

Figure 3 shows the time evolution of the step pattern (growing in the [01] direction) induced by the linear adatom source moving at the velocity $V_p = 0.02$. From the kink energy, approximate values of the step stiffness of a (01) step and a (11) step (for a solid-on-solid model) are calculated as[8]

$$\frac{\tilde{\beta}_{[01]}}{k_B T} = \frac{(1 - e^{-\epsilon/k_B T})^2}{2e^{\epsilon/k_B T}}, \tag{3}$$

$$\frac{\tilde{\beta}_{[11]}}{k_B T} = \sqrt{2}\frac{(1 - e^{-2\epsilon/k_B T})^2}{(1 + e^{-2\epsilon/k_B T})^2 + 4e^{-2\epsilon/k_B T}}. \tag{4}$$

(The general exact value for a step in the Ising model is given in Ref. 25.) When the kink energy is set to $\epsilon/k_B T = 2.0$, which is the standard value in our simulation, the step stiffnesses are $\tilde{\beta}_{[01]}/k_B T = 2.76$ and $\tilde{\beta}_{[11]}/k_B T = 1.23$, respectively. Initially, the source is close to the step, and adatoms released from the source almost immediately solidify and make the step rough. At $t = 500$, step wandering with a characteristic wavelength becomes visible [Figs. 3(a) and 3(b)]. As the source leaves the step behind, the density gradient of adatoms makes the step linearly unstable. Fluctuations of short wavelengths are stable so that small corrugations decay. Only fluctuations of linearly unstable modes grow, and the fingerlike protrusions appear at $t = 2500$ [Fig. 3(c)]. After a competition of growing fingers, less than half the growing fingers seem to survive, and they start to make branches at $t = 5000$ [Fig. 3(d)].

Figures 4(a) and 4(b) show developed step patterns with the source velocity $V_p = 0.01$. In contrast to the usual wandering patterns, the step forms fingerlike branches. Since the growth direction of the (01) step is the stiffest orientation of a step, frequent tip splitting and branching occur in the [01] growth [Fig. 4(a)]. The branches tend to grow tilted directions of smaller stiffnesses. Eventually, a forest pattern consisting of treelike protrusions is formed. In contrast, since stiffness is smallest in the [11] direction, branching occurs less frequently, and most branches grow upward [Fig. 4(b)].

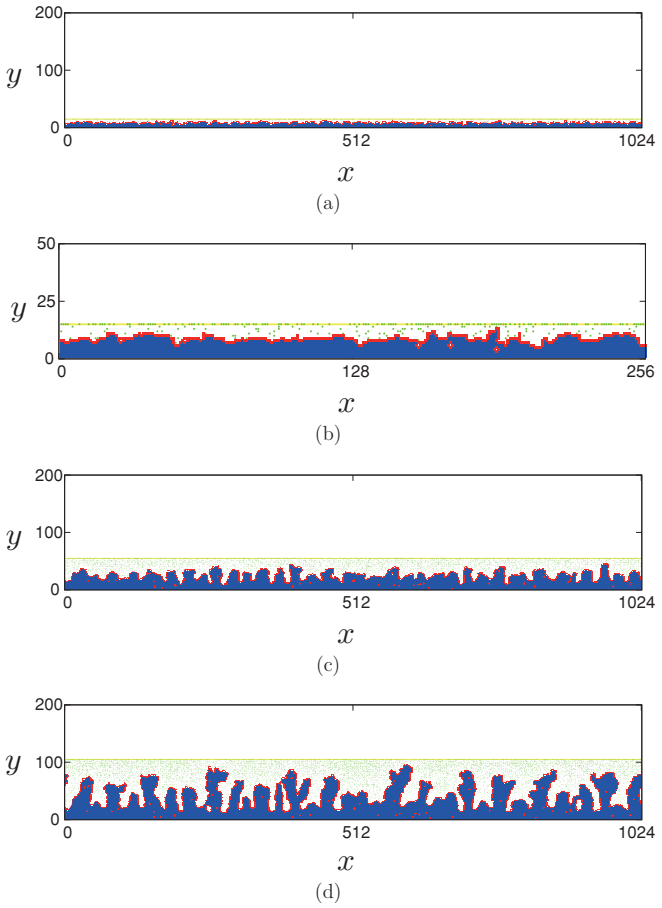

FIG. 3. (Color online) Time evolution of the step growing in the [01] direction with the source velocity $V_p = 0.02$ at (a) $t = 500$, (b) a four times magnified view of (a), (c) $t = 2500$, and (d) $t = 5000$. Blue and red (dark area) represent solid and step atoms, and green (gray) dots represent adatoms.

In most grown areas, the solid layer occupies half the terrace, which is covered with adatoms of the equilibrium density, as expected from the conservation law.

IV. SOURCE SPEED AND CHARACTERISTIC LENGTH

In the experiment of Si,[21] the velocity of the phase boundary, i.e., the velocity of the source, decreases with decreasing the deposition rate of the Ga atoms. Figures 4(c) and 4(d) show patterns with a slower source velocity. The patterns do not change much from Figs. 4(a) and 4(b), but the characteristic length becomes longer. The formation of side branches in the (11) step hardly occurs, and the pattern is similar to the pattern observed in the experiment (Fig. 1). In step wandering instabilities, the period of step pattern is usually characterized by the wavelength of the fastest growing mode λ_{max}, obtained from a linear stability analysis. Because of the conservation of atoms, any steady state of a straight step with the moving source is not possible unless $c_0 = 1$,[26] and the linear stability analysis cannot be made here.

In a previous study,[27] we used another model in which a linear reservoir with a constant adatom density was introduced. The distance between the step and the reservoir was controlled in the MC simulation. The model was intended to make

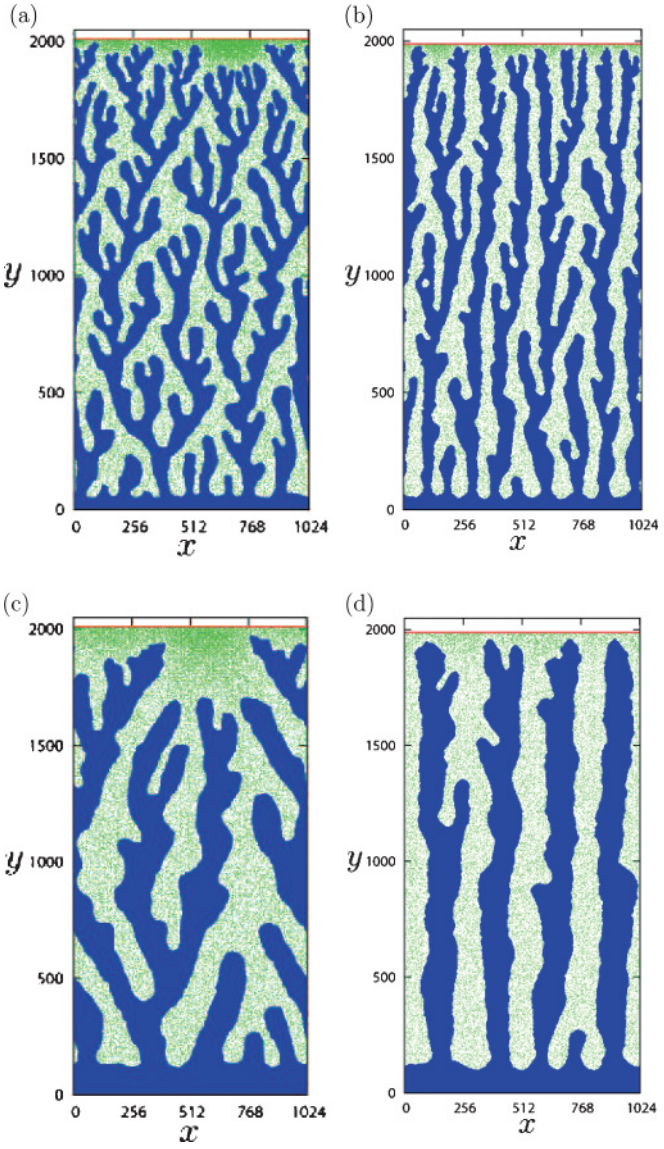

FIG. 4. (Color online) Step patterns induced by the linear source (red line on top) of atoms at the velocity $V_p = 0.01$, (a) in the [01] direction and (b) in the [11] direction, and $V_p = 0.002$, (c) in the [01] direction and (d) in the [11] direction. Blue (dark gray) represents the solid layer, and green (light gray) dots represent adatoms.

a comparison with the linear stability analysis possible by keeping the diffusion length l_D constant.[28] Fingerlike patterns similar to Fig. 4 were also observed. In this model, the linear amplification rate ω_q of the step fluctuation is obtained as

$$\frac{\omega_q}{D_s} \approx |q| \left(\frac{1}{l_D} - \frac{\Gamma q^2}{1 - c_{eq}^0} \right), \tag{5}$$

where D_s is the diffusion coefficient and $\Gamma = c_{eq}^0 \tilde{\beta} / k_B T$ is the capillary length (note that the lattice constant is set to be unity). The wavelength of the fastest growing mode is given by

$$\lambda_{max} = 2\pi \sqrt{\frac{3\Gamma l_D}{1 - c_{eq}^0}}, \tag{6}$$

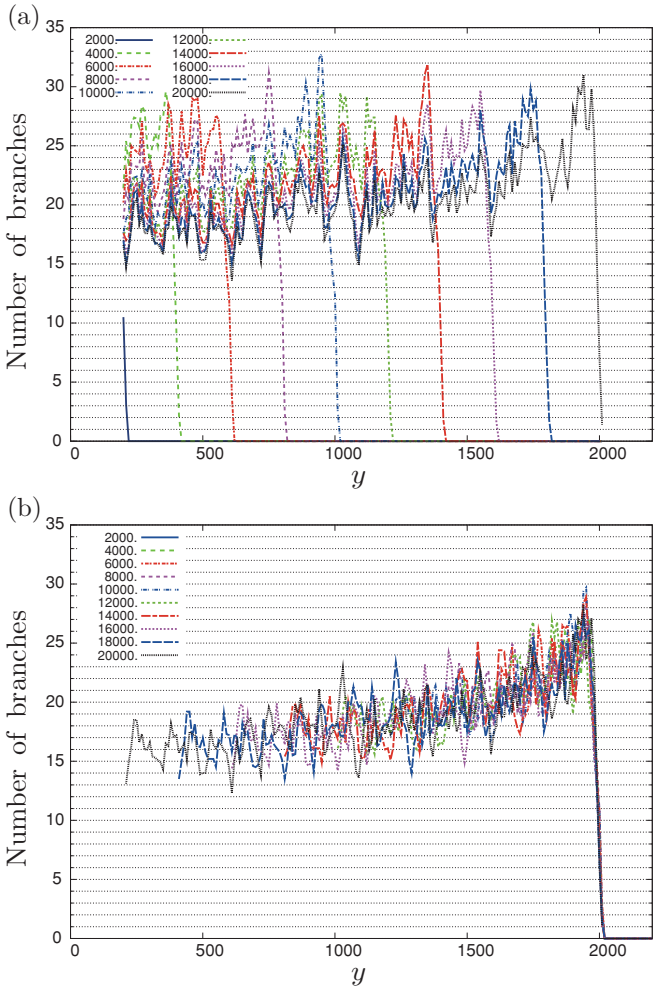

FIG. 5. (Color online) (a) Profiles of the number of steps as a function of the position at several different times (t = 2000,4000, . . . ,20 000) with $V_p = 0.1$ and $\epsilon/k_BT = 2.0$. (b) Shifted profiles of (a) to align the step front. The width of the system is 1024.

which was confirmed in the previous simulation for the initial stage of the instability. Although the diffusion length is not controlled, the present model has better correspondence with the experiment and is much simpler. If we relate the diffusion length l_D and the source velocity V_p as $l_D = D_s/V_p$, the dependence of the period of the pattern may be the same as that in the previous model.[27] Then, we may compare the typical period of branches with Eq. (6).

We count the number of steps cut by a horizontal line over the system width and determine the typical period of branches. To count the number, we have eliminated both step atoms that enclose a vacancy in the solid area and projections or dents comparable to the lattice size. Figure 5(a) shows profiles of the number of branches as a function of position y. Although they are changing in time, the shifted profiles shown in Fig. 5(b) indicate that the step pattern is roughly steady in the moving frame with the step front (equivalently, with the source). Note that the pattern cannot be steady if one looks at the connectivity of the branches since surviving trees become fewer and fewer as they grow. Only the number of branches makes the steady profile.

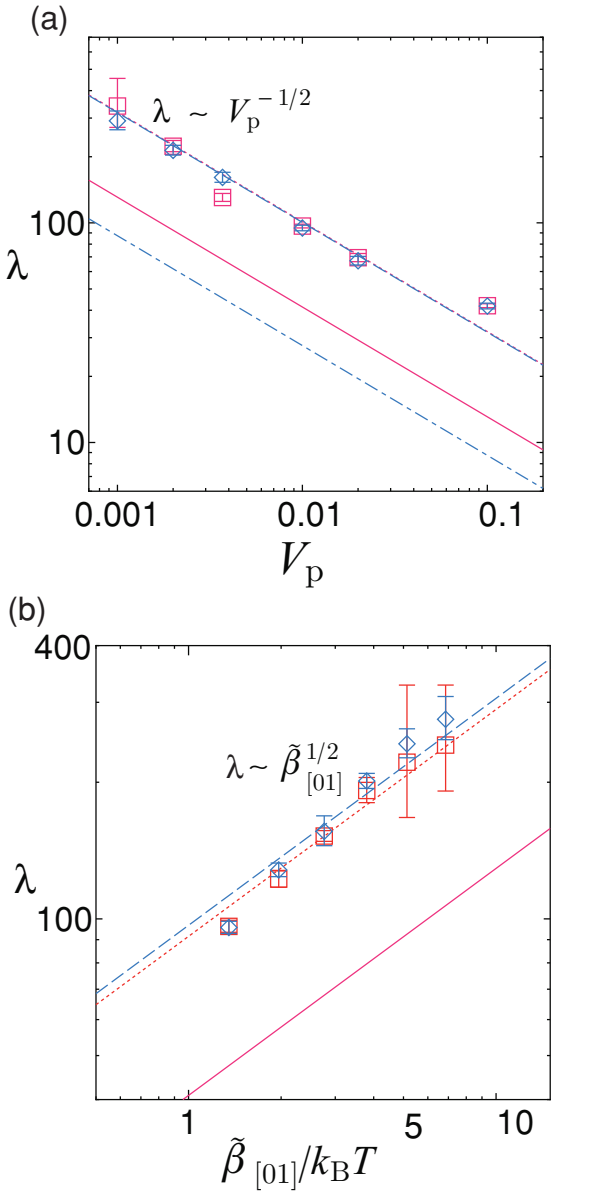

FIG. 6. (Color online) (a) Dependence of period λ of the branches on the source velocity V_p, with $\epsilon/k_BT = 2.0$. The data are averaged over nine different times for ten independent runs. (b) Dependence of λ on the stiffness $\tilde{\beta}_{[01]}$ with $V_p = 0.0037$. □, (01) step; ♢, (11) step; solid line, λ_{max} with $\tilde{\beta}_{[01]}$; dotted broken line, λ_{max} with $\tilde{\beta}_{[11]}$; and other lines, fits to the data with slope 1/2.

Figure 6(a) shows the relation between the period of branches (measured at the peak position in profiles, such as Fig. 5) λ and the source velocity V_p. The apparent relation $\lambda \sim V_p^{-1/2} \sim l_D^{1/2}$ agrees with Eq. (6), but the observed period is about 2.4 times longer for a (01) step [and 3.6 times longer for a (11) step] than λ_{max}.

Despite the different appearance in the (11) step compared with the (01) step, the period of branches is about the same, as shown in Fig. 6(a). The characteristic wavelength of the initial instability is probably determined by Eq. (6) as in the case of a constant diffusion length,[27] but the characteristic wavelength of the developed pattern hardly depends on the growth direction. In Fig. 6(b), we show the period of branches

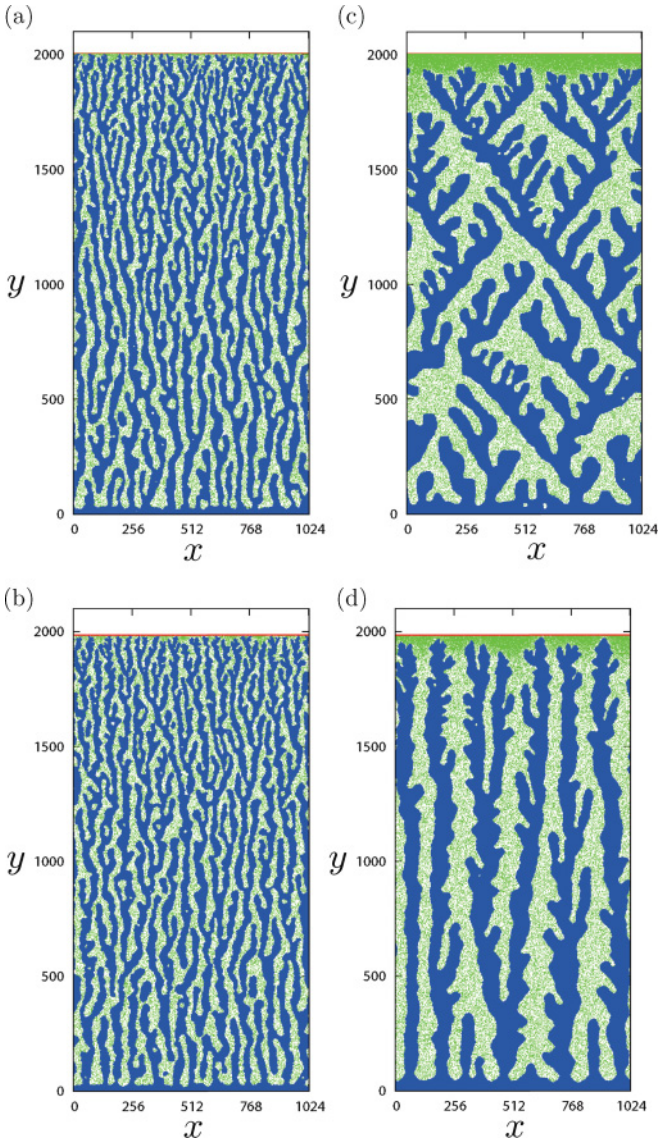

FIG. 7. (Color online) Step patterns with various stiffnesses ($V_p = 0.02$). (a) $\tilde{\beta}_{[01]} = 1.35$ ($\epsilon/k_BT = 1.5$) and (b) $\tilde{\beta}_{[01]} = 5.13$ ($\epsilon/k_BT = 2.5$) in the [01] direction. (c) $\tilde{\beta}_{[11]} = 0.98$ ($\epsilon/k_BT = 1.5$) and (d) $\tilde{\beta}_{[11]} = 1.34$ ($\epsilon/k_BT = 2.5$) in the [11] direction.

as a function of the stiffness in the [01] direction $\tilde{\beta}_{[01]}$. The square-root dependence of λ on $\tilde{\beta}_{[01]}$ agrees with Eq. (6).[29] The corresponding step patterns with small and large stiffnesses are shown in Fig. 7. The tendency to grow into the less stiff directions is evident. Thus, among unstable step fluctuations of various wavelengths, the characteristic wavelength λ selected is controlled by the capillary length Γ of the [01] direction and the diffusion length l_D defined by the source velocity V_p. As a result of competition of branches and local relaxation, the characteristic length λ becomes more than twice as large as λ_{max} of Eq. (6).

V. ADJUSTMENT OF VELOCITY AND FRACTAL PATTERNS

In Figs. 4 and 7, wandering instability is induced by the gradient of the adatom density in front of the step, and the step shows a treelike pattern growing steadily. We can interpret the result as follows: The step changes its shape from the straight one to the treelike one in order to follow the moving linear source and realizes the steady state by adjusting the characteristic length λ. Since the stiffness is large in the [01] direction, branches tend to grow into the soft directions of small stiffnesses, i.e., in the $\langle 11 \rangle$ directions. Therefore, for the (01) step, successive branching of protrusions is inevitable [Figs. 4(a), 4(c), 7(a), and 7(b)]. For the (11) step, the stiffness is smaller, and protrusions grow with less branching [Figs. 4(b), 4(d), 7(c), and 7(d)]. These patterns for the trees with branch period $\lambda \sim \sqrt{\Gamma l_D}$ are consistent with the adatom distribution set by velocity V_p of the source and are selected in the steady state.

When velocity V_p of the source is increased, the step adjusts its characteristic length λ to the shorter diffusion length, and consequently, the step can follow the source. However, this mechanism breaks down if the source escapes too fast. When the characteristic length becomes small, relative strength of random fluctuation increases, and the pattern resembles a random-growth pattern in a diffusion field:[30] such growth from a finite-density gas is known to make a fractal pattern.[31] In the fractal growth without melting, diffusion length l is related to an upper cutoff length of the fractal structure. It is controlled by fractal dimension d_f of the diffusion-limited aggregation (DLA) and density c of the adatom gas. It should be noted that, once the step fails to follow the source, the diffusion length is no longer related to the source velocity. To realize a steady state in the fractal growth, the number conservation requires that the average density of the fractal solid within l should be the adatom density away from the step, $l^{d_f}/l^d \approx c$ where d is the spatial dimension. Therefore, the growth velocity of the DLA-like pattern is determined by the diffusion length as

$$V_{DLA} \sim \frac{D_s}{l} \sim c^{1/(d-d_f)}. \tag{7}$$

For the present case of a two-dimensional adatom gas, the exponent is 3.5 with $d_f = 1.71$ and $d = 2$. Breakdown of the pattern adjustment occurs when V_p exceeds critical velocity V_D, which is an analog of Eq. (7) so that the step is no longer able to follow the escaping source.

Figure 8 shows a DLA-like step pattern when the source moves too fast. The step grows at a constant velocity $V_D \approx 0.16$ independent of V_p, and a large area of the uniform adatom density $c = c_0 = 0.525$ is left behind the linear source moving at the top. The pattern is similar to the fractal growth found in Ref. 31. Actually, if $\phi \to \infty$ and $V_p \to \infty$, solidification becomes irreversible, and the present model is identical to the fractal growth model of Ref. 31. Figure 9(a) shows the dependence of growth velocity V_s (velocity of the top of the step) on V_p with various c_0. If V_p is smaller than V_D, which is about 0.16 for $c_0 = 0.525$, as indicated by the squares in Fig. 9(a), the step follows the source at velocity V_p. If V_p is larger than V_D, the step cannot follow the source, and the growth velocity is constant $V_s = V_D$. The transition between the two modes is abrupt. In Fig. 9(b), we show the dependence of V_D on an effective excess density Δc_0. In order to subtract the background of the equilibrium density, the effective excess

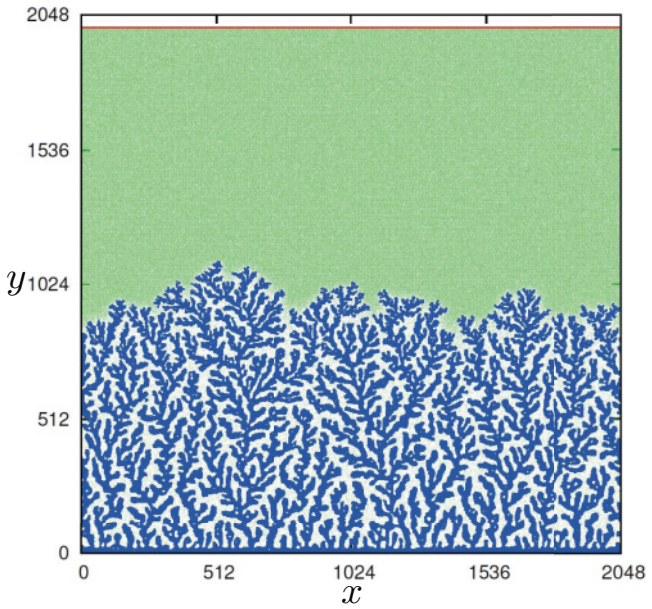

FIG. 8. (Color online) Step pattern at $V_p = 1$ resembles the fractal growth from a finite-density gas.[31] $\phi/k_BT = 3.0$ and $\epsilon/k_BT = 2.0$.

density is defined by

$$\Delta c_0 \equiv \frac{c_0 - c_{eq}^0}{1 - c_{eq}^0}, \tag{8}$$

which is the areal ratio of the solid in the grown area. Finiteness of ϕ in the present model allows melting, and branches become thicker. As a result, velocity V_D [circles in Fig. 9(b)] is slower than velocity V_{DLA} of the irreversible fractal growth [diamonds in Fig. 9(b)]. The relation of the growth velocity to the density, however, shows the same behavior, $V_D \sim (\Delta c_0)^{3.5}$.

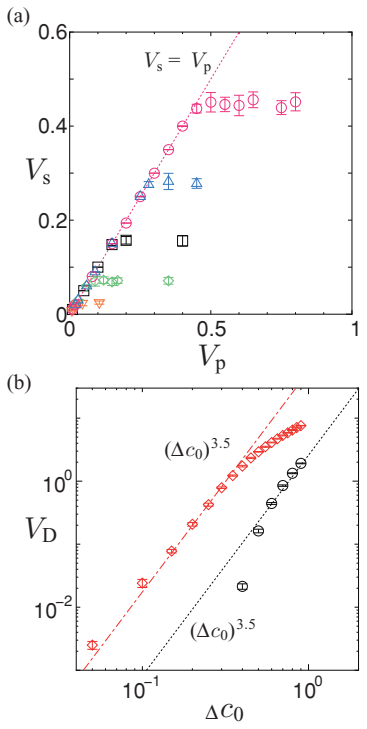

FIG. 9. (Color online) (a) Dependence of growth velocity V_s on the velocity of linear source V_p. Excess adatom densities Δc_0 are ▽, 0.4; ◇, 0.45; □, 0.5; △, 0.55; and ◯, 0.6. (b) Dependence of V_D on Δc with $\phi/k_BT = 3.0$ (◯) and with $\phi \to \infty$ (◇).

VI. SUMMARY

We studied pattern formation of a step induced by a moving linear source of adatoms. Initially, due to high adatom density at the step, the step becomes rough, and small projections and dents are formed at the beginning. The balance between the destabilizing effect of diffusion and the stabilizing effect of stiffness selects a characteristic length $\lambda \sim \sqrt{\Gamma l_D}$. After competition of intrusions, survived ones grow and form branches and trees. Soon a treelike step follows the source, and a steadily growing state is realized. The branching pattern depends on the crystal anisotropy. A comblike pattern with few branches may be formed in the ⟨11⟩ growth. The pattern is similar to that observed on a Si(111) surface with Ga deposition.[21] The change in λ as the change in the source velocity agrees with the change as the deposition rate in the experiment. The period of branches in the steady state of simulation is about 2.4 times λ_{max} expected from the linear stability analysis with the stiffness in the [01] direction for both (01) and (11) steps. If velocity V_p of the source is increased, the characteristic length is adjusted to follow the source. Above critical velocity V_D, which is determined by fractal dimension d_f of the DLA and adatom density c_0, the step grows at the critical velocity, independent of V_p.

Recently, the comblike step pattern was observed during epitaxial growth of graphene on SiC. When SiC is heated at a high temperature, Si atoms are evaporated, and a buffer layer of a carbon-rich $6\sqrt{3} \times 6\sqrt{3}$ structure is formed. With further evaporation of Si, a new buffer layer is formed, and the existing buffer layer becomes graphene. The formation of a fingerlike graphene pattern is observed in the lower side near the step, which is the source of the C atoms.[32–34] The number of C atoms in graphene is almost equal to that in three SiC bilayers. Therefore, if C atoms emitted from a retreating triple-bilayer step are immediately consumed to form graphene, the growth front of graphene could follow the retreating step.[34] On the other hand, retreating single- or double-bilayer steps cannot supply C atoms sufficient to form graphene over the whole retreated area. Although a detailed mechanism is not clear yet, it seems that such insufficient C supply causes the fingerlike graphene pattern.[34] Then, the present mechanism may also explain the formation of the fingerlike pattern of graphene on SiC.

In our simulation, the dependence of the period of branches λ on Γ and V_p agrees with the linear stability analysis, but, owing to competition between branches, coarsening occurs and period λ is several times larger than λ_{max}. Now, we are investigating the coarsening process in more detail.

ACKNOWLEDGMENTS

The work was supported by Grants-in-Aid from the Japan Society for the Promotion of Science. M. U. thanks N. C. Bartelt and T. Ohta for informative discussions on graphene growth.

*uwaha@nagoya-u.jp

[1]For a theoretical review, C. Misbah, O. Pierre-Louis, and Y. Saito, Rev. Mod. Phys. **82**, 981 (2010).
[2]For an experimental review, K. Yagi, H. Minoda, and M. Degawa, Surf. Sci. Rep. **43**, 45 (2001).
[3]R. L. Schwoebel and E. J. Shipsey, J. Appl. Phys. **37**, 3682 (1966).
[4]G. Ehrlich and F. G. Hudda, J. Chem. Phys. **44**, 1039 (1966).
[5]R. L. Schwoebel, J. Appl. Phys. **40**, 614 (1969).
[6]G. S. Bales and A. Zangwill, Phys. Rev. B **41**, 5500 (1990).
[7]I. Bena, C. Misbah, and A. Valance, Phys. Rev. B **47**, 7408 (1993).
[8]M. Uwaha and Y. Saito, Phys. Rev. Lett. **68**, 224 (1992); Y. Saito and M. Uwaha, Phys. Rev. B **49**, 10677 (1994).
[9]Y. Kuramoto and T. Tsuzuki, Prog. Theor. Phys. **55**, 356 (1976).
[10]G. I. Sivashinsky, Acta Astronaut. **4**, 1177 (1977).
[11]Y. Saito and M. Uwaha, J. Phys. Soc. Jpn. **65**, 3576 (1996).
[12]O. Pierre-Louis, C. Misbah, Y. Saito, J. Krug, and P. Politi, Phys. Rev. Lett. **80**, 4221 (1998).
[13]F. Gillet, O. Pierre-Louis, and C. Misbah, Eur. Phys. J. B **18**, 519 (2000).
[14]M. Sato, M. Uwaha, Y. Saito, and Y. Hirose, Phys. Rev. B **65**, 245427 (2002).
[15]R. Kato, M. Uwaha, Y. Saito, and H. Hibino, Surf. Sci. **522**, 64 (2003).
[16]M. Sato, M. Uwaha, Y. Saito, and Y. Hirose, Phys. Rev. B **67**, 125408 (2003).
[17]A. V. Latyshev, A. L. Aseev, A. B. Krasilnikov, and S. I. Stenin, Surf. Sci. **213**, 157 (1989).
[18]M. Sato and M. Uwaha, J. Phys. Soc. Jpn. **65**, 2146 (1996).
[19]M. Degawa, H. Nishimura, Y. Tanishiro, H. Minoda, and K. Yagi, Jpn. J. Appl. Phys., Part 2 **38**, L308 (1999).
[20]M. Sato, M. Uwaha, and Y. Saito, Phys. Rev. Lett. **80**, 4233 (1998).
[21]H. Hibino, H. Kageshima, and M. Uwaha, Surf. Sci. **602**, 2421 (2008).
[22]The advantage of introducing the two parameters[8] ϵ and ϕ is that we can independently change the step stiffness and the equilibrium adatom density.
[23]If the step edge diffusion barrier is large, this assumption is justified on a real vicinal face.
[24]The balance of the number of atoms between the initial state and the final state is $c_0 = x + c_{\rm eq}^0(1-x)$, where x is the portion of the solid area. That is, $0.525 = 1 \times 0.5 + 0.05 \times (1-0.5)$, in the present case.
[25]C. Rottman and M. Wortis, Phys. Rev. B **24**, 6274 (1981); J. E. Avron, H. van Beijeren, L. S. Schulman, and R. K. P. Zia, J. Phys. A **15**, L81 (1982); Y. Akutsu and N. Akutsu, *ibid.* **19**, 2813 (1986).
[26]Y. Saito, *Statistical Physics of Crystal Growth* (World Scientific, Singapore, 1996).
[27]M. Sato, S. Kondo, and M. Uwaha, J. Cryst. Growth **318**, 14 (2011).
[28]The diffusion length is defined by $l_{\rm D} = l \ln[(1-c_{\rm eq}^0)/(1-c_{\rm R})]$, where $c_{\rm R}$ is the density of the reservoir and l is the distance between the step and the reservoir. This relation is derived from the density distribution in a steady state.
[29]The parameter actually changed in the simulation is kink energy $\epsilon/k_{\rm B}T$, and both $\tilde{\beta}_{[01]}$ and $\tilde{\beta}_{[11]}$ change accordingly. Only the relation between $\tilde{\beta}_{[01]}$ and λ shows the simple behavior.
[30]T. Vicsek, *Fractal Growth Phenomena* (World Scientific, Singapore, 1992).
[31]M. Uwaha and Y. Saito, J. Phys. Soc. Jpn. **57**, 3285 (1988); Phys. Rev. A **40**, 4716 (1989).
[32]V. Borovikov and A. Zangwill, Phys. Rev. B **80**, 121406(R) (2009).
[33]M. L. Bolen, S. E. Harrison, L. B. Biedermann, and M. A. Capano, Phys. Rev. B **80**, 115433 (2009).
[34]T. Ohta, N. C. Bartelt, S. Nie, K. Thürmer, and G. L. Kellogg, Phys. Rev. B **81**, 121411(R) (2010).